The Journal of International Advanced Otology

J Int Adv Otol 2021; 17(1): 35–41 • DOI: 10.5152/iao.2020.9384

Original Article

Superior Semicircular Canal Dehiscence by Superior Petrosal Sinus: Proposal for Classification

Eugen Ionescu, Pierre Reynard, Aurélie Coudert, Lucian Roiban, Aïcha Ltaief Boudrigua, Hung Thai-Van

Department of Audiology and Neurotology, Hospices Civils de Lyon, Lyon, France (EI, PR, HTV)
Paris Hearing Institute, Institut Pasteur, Paris, France (EI, PR, HTV)
Claude Bernard Lyon 1 University, Lyon, France (PR, HTV)
Department of Otolaryngology – Head & Neck Surgery, Edouard Herriot Hospital - Hospices Civils de Lyon, Lyon, France (AC)
Integrative Multisensory Perception Action & Cognition Team — ImpAct, Lyon Neuroscience Research Center, Lyon, France (AC)
Univ Lyon, INSA-Lyon, CNRS, UCBL, MATEIS, UMR 5510, Villeurbanne, France (LR)
Department of Radiology, Hospices Civils de Lyon, Lyon, France (ALB)

Cite this article as: Ionescu E, Reynard P, Coudert A, Roiban L, Ltaief Boudrigua A, Thai-Van H. Superior Semicircular Canal Dehiscence by Superior Petrosal Sinus: Proposal for Classification. J Int Adv Otol 2021; 17(1): 35-41.

OBJECTIVES: This study aimed to present 3 different clinical stages in patients presenting with superior semicircular canal dehiscence (SSCD) by the superior petrosal sinus (SPS). A specific 3-class classification based on clinical, radiological, and audio-vestibular arguments is proposed.

MATERIALS AND METHODS: We retrospectively compared clinical and radiological findings in 3 patients with different degrees of audio-vestibular dysfunction in whom the imagery evocated the diagnosis of SSCD by SPS. Imaging sensitivity was improved by combining inner ear high-resolution computed tomography (HRCT) scan and magnetic resonance imaging in fusion, allowing us to compare and corroborate clinical and audio-vestibular findings in each case with the imagery.

RESULTS: HRCT and 3T inner ear fusion imaging highlighted a direct contact and/or compression between SPS and the membranous superior semicircular canal (SSC). We propose a new classification of SSCD by SPS. Class "A" corresponds to an HRCT image with a "cookie bite" and thin bone still covering the SSC. Class "B" corresponds to a "cookie bite" image with confirmed contact between the SPS wall and the membranous SSC in MRI labyrinthine sequences. Class "C" type corresponds to a "cookie bite" image, contact, and obvious compression of the membranous SSC by SPS on MRI sequences.

CONCLUSION: Anatomical systematization is needed for daily practice. This classification of SSCD by SPS would contribute to a better understanding of the wide variety and variability in the occurrence and onset of symptoms.

KEYWORDS: Superior semicircular canal dehiscence, superior petrosal sinus, otic capsule vascular-type dehiscence

INTRODUCTION

Third window (TW) abnormalities correspond to defects in the bony structure of the otic capsule, which locally reduce the hydrodynamic resistance of the perilymphatic space (PS) [1]. This explains a lower compliance gradient of the vestibular membrane that facilitates a deviation of the normal perilymphatic flow toward the location of the abnormal window [2-6]. When the TW is located in the cochlear part of the PS between the oval and round windows, the expected consequences could lead to a conductive or a mixed hearing loss. When the abnormal window is located in the vestibular part of the PS, a vestibular co-stimulation by loud sounds could occur. The explanation is that the hydraulic force exerted by the perilymph flow is not fully directed toward the basilar membrane and the organ of Corti as it should be but is also directed posteriorly toward the vestibular compartment [4, 6]. This abnormal vestibular co-stimulation, known as the Tullio phenomenon is one of the main clinical signs [1-5] in patients with TW anomalies, also called otic capsule dehiscence (OCD) syndrome as described by Wackym et al. [7] OCD refers to all TW spectrum disorders whose symptoms and signs on physical examination and audiological findings are common. Because of the progressive increase in reported variants, the identification of the anatomical structures involved at the TW interface is essential to assess the vestibular end organ that is likely to cause an abnormal response or perception and therefore to select the most appropriate treatment.

This study was presented at the 30th Congress Bárány Society Meeting, June 10-13, 2018, Uppsala, Sweden.

Corresponding Address: Pierre Reynard E-mail: pierre.reynard@hotmail.fr

Submitted: 08.25.2020 • **Revision Received:** 09.22.2020 • **Accepted:** 10.02.2020
Available online at www.advancedotology.org

Our department currently uses an anatomically based systematization of OCD with 4 types according to the engaged anatomic structures at the TW interface: (1) meningeal/vestibular (or classic SSCD); (2) vascular (e.g., superior petrosal sinus (SPS), internal jugular vein, or internal carotid artery)/vestibular; (3) petrosal air cells system (e.g., epitympanic cavity, facial nerve canal)/vestibular, (4) and the vestibular/vestibular (e.g., endolymphatic sac, enlarged vestibular aqueduct). The most common variant of the upper semicircular canal dehiscence (OCD) as found in Minor's syndrome is medially localized, being in contact with the frontobasal dura mater. More rarely, SSCD is located posteromedially involving the SPS [8, 9]. This study focused on this particular vascular type of OCD in which the SPS is engaged.

High-resolution computed tomography (HRCT) with infra-millimetric reconstructions in the Pöschl plane are essential for TW diagnosis. If HRCT is not routinely performed as recommended [10, 11], the diagnosis can easily be missed. HRCT in association with lower than normal threshold cervical vestibular evoked myogenic potentials (cVEMPs) are historically the golden standard tests in this pathology [12, 13]. Based on the HRCT criteria, Lookabaugh et al. [9] proposed a classification of the SSCD into 6 types. Sweeney et al. [14] proposed another classification of SSCD by SPS into 4 categories, taking into account the relationship between SSC, the SPS, and/or the subtemporal dura mater of the middle cranial fossa. The interest in observing a "true" contact between the SSC and the SPS and the relationship between the dehiscent otic capsule and the neighboring structures was recently highlighted by Ozgur et al. [15] According to this research and on the basis of our recent experience, fusion imaging between petrosal bone HRCT in the Pöschl plane and 3D T1 vascular MRI sequences highlighted with precision the contact between the petrosal venous wall and the membranous semicircular canal [15,16]. In this paper, we aimed to present clinical and radiological arguments to support the value of using high-resolution 3T MRI sequences on the inner ear alongside petrosal bone HRCT to highlight a possible contact and/or a compression effect of the SPS on the membranous SSC.

MATERIALS AND METHODS

Population

Over a period of 3 years, all symptomatic patients with OCD by SPS were recruited. Only 10 patients with a complete clinical and radiological analysis (HRCT and MRI) were studied for this classification.

Clinical and Audiological Assessment

Standard ENT examination including cranial nerve assessment and oto-microscopy were routinely performed in each patient. Pure tone audiometry (PTA; Madsen Astera-Otometrics) middle ear reflexes (Madsen Zodiac 901 tympanometer), videonystagmography (VNG, Ulmer System®; Synapsis SA), video head impulse test (VHIT, ICS Impulse®; GN Otometrics), and cVEMPs (Bio-Logic® Nav-Pro system) in air conduction with 750 Hz tone bursts stimuli were systematically performed in all patients. Protocols similar to our previous study [16] were adopted. The VNG protocol systematically included the skull vibration-induced nystagmus test (VINT) at 100 Hz (bone vibrator VVIB 100 Hz Synapsys, France) [17]. Tinnitus Handicap Inventory (THI) and Dizziness Inventory Handicap (DHI) questionnaires adapted to French language were collected from each patient [18, 19]. The 3 functional degree DHI scale proposed by Jacobson et al. [18] was used as following: mild (16–34 points), moderate (36-52 points), and severe impairment (>54 points). THI scores were classified according to the impact of the disability on a daily basis as following: no impact (0-16), mild (18-36), moderate (38-56), severe (58-76), and catastrophic (above 78) [19].

Radiological Assessment

High Resolution Cranial Tomodensitometry (GE GSI Revolution, GE Healthcare, United States) of the petrous bone was performed in all patients. Slices were acquired helically in the axial plane at a nominal 0.625 mm slice thickness with a 50% overlap of 0.312 mm as recommended [10, 11]. Images were obtained in ultrahigh resolution at 140 kV and 200 mAs/section. The primary images were retargeted to the axial and coronal planes of the lateral semicircular canal to a 60 mm field of view with a 512 matrix for an isometric voxel. The retargeted axial scans were then reformatted in the Pöschl plane, using AW Server software (GE Healthcare, United States).

Additionally, 3T MRI of the petrosal bone and inner ear structures was also performed in all patients (GE 3T MRI, GE Healthcare; and Philips Ingenia 3T MRI, Philips healthcare). Particularly, 3D T1 weighted sequences were used to show SPS opacification and labyrinthine sequence 3D T2 high-resolution FIESTA (Fast Imaging Employing STeady state Acquisition) or DRIVE (DRIVen Equilibrium pulse, TE 157, TR 1000, slices thickness 0.4, Turbo factor 40, Matrice 500 x 500, voxel size: 0.4 x 0.4 isotropic) were used to show the membranous labyrinth morphology and patency. Fusion imaging between HRCT Pöschl plane and 3D T1 weighted enhanced sequence was performed using a post processing software (AW Server, GE Healthcare). The resulting images allowed for a good evaluation of the TW's interface (e.g., dimensions of the SPS, interface surface, or contact surfaces between vestibular membrane(s) and the walls of the SPS, and an eventual compression effect on the membranous SSC). We assume that this approach is superior to the "classic" HRCT of the temporal bone, which may incidentally show typical "cookie bite" images [20], including in asymptomatic patients.

MAIN POINTS

- Whereas the most common variant of the upper semicircular canal dehiscence (Minor's syndrome) is anatomically localized on its medial part, SSCD involving the sinusal posterior sinus (SPS) is located more posteriorly, closer to its cupulae.
- The combination of petrosal bone HRCT and labyrinthine 3T MRI techniques allowed for visualizing either a simple contact or a compression generated by the SPS on the membranous SSC duct.
- A 3-class classification of the SSCD by SPS was proposed to select patients needing surgical or endovascular treatment.
- In authors' opinion, this classification allows a better comprehension of the vestibular/vascular dehiscence type.

RESULTS

We therefore proposed a classification of OCDS by SPS into 3 classes as shown in Table 1. Each class was highlighted by a clinical report (Figures 1, 2, and 3).

Table 1. Clinical-radiological classification of the SSCD by SPS

SSCD by SPS	Combined HRCT & MRI findings Audiological and clinical findings
Class A (Figure 1)	- "cookie bite" HRCT image with a thin bone covering the SSC ("near dehiscence"); no contact between the SPS and the membranous SSC on labyrinthine 3T MRI sequences. - No CHL; normal cVEMPs thresholds. - Patient 1: non symptomatic.
Class B (Figure 2)	- "cookie bite" HRCT image with limited contact on MRI labyrinthine 3T between the SPS and the membranous SSC (or slight indentation on PS only). - Patient 2: limited low frequency CHL and lower than normal cVEMPs threshold. - The patient was mildly impaired.
Class C (Figure 3)	- "cookie bite" HRCT with SSCD in HRCT, evident contact and compression of the membranous SSC by the SPS (and also probable indentation on the ES). - Patient 3: low frequency CHL with better than expected BC, and lower than normal cVEMPs threshold. - The patient was severely impaired.

SSCD: Superior semicircular canal dehiscence; SPS: Superior petrosal sinus; HRCT: high-resolution computed tomography; CHL: conductive hearing loss; BC: bone conduction; cVEMP: cervical vestibular evoked myogenic potential; PS: perilymphatic space; ES: endolymphatic sac.

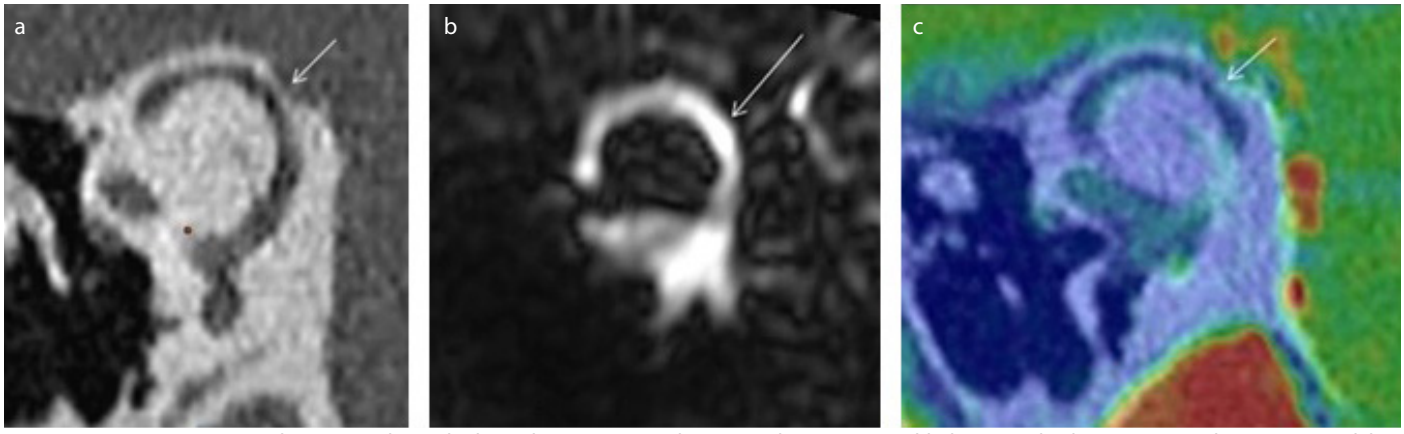

Figure 1. a-c. Case report 1– Class A. a) right ear high-resolution computed tomography (HRCT) Pöschl plane. "Cookie bite" corresponding to a "near dehiscence"; a thin bone covering the membranous SSC is observed (white arrow). b) T2 HR DRIVE; superior semicircular canal (SSC) membrane in Pöschl plane. and c) Fusion between HRCT and 3D T1 weighted enhanced sequences. b) and c) images show no contact between the membranous SSC and superior petrosal sinus (SPS). Arrows indicate the SPS at a distance from the membranous SSC with no contact between the two structures.

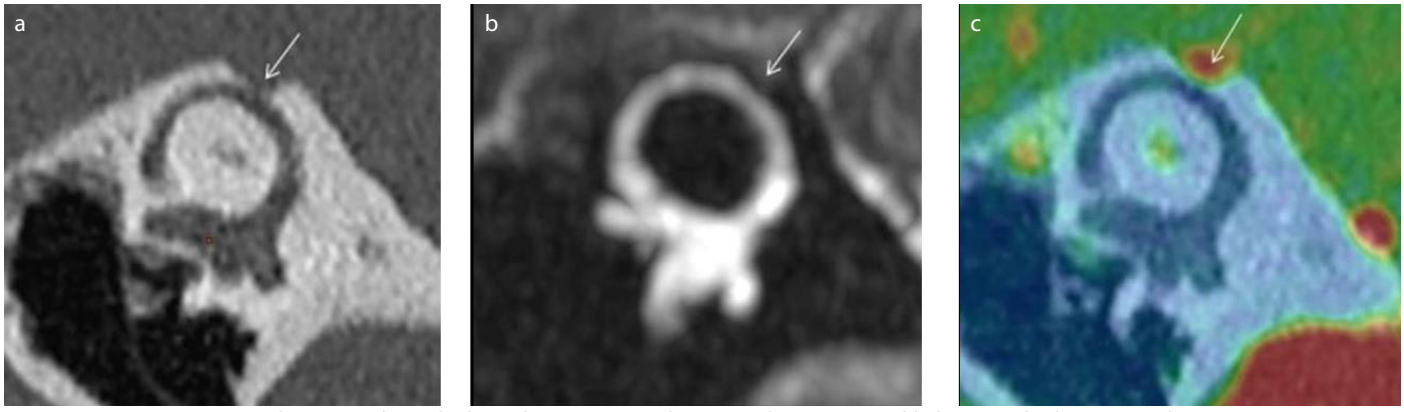

Figure 2. a-c. Case report 2 – Class B. a) right ear high-resolution computed tomography (HRCT) Pöschl plane. "Cookie bite" aspect. b) T2 HR FIESTA sequence: vascular structure (arrow) in contact with the membranous SSC. c) Fusion between HRCT and 3D T1 weighted enhanced sequences: limited contact between superior petrosal sinus (SPS) (arrow) and membranous superior semicircular canal, without evident labyrinthine compression.

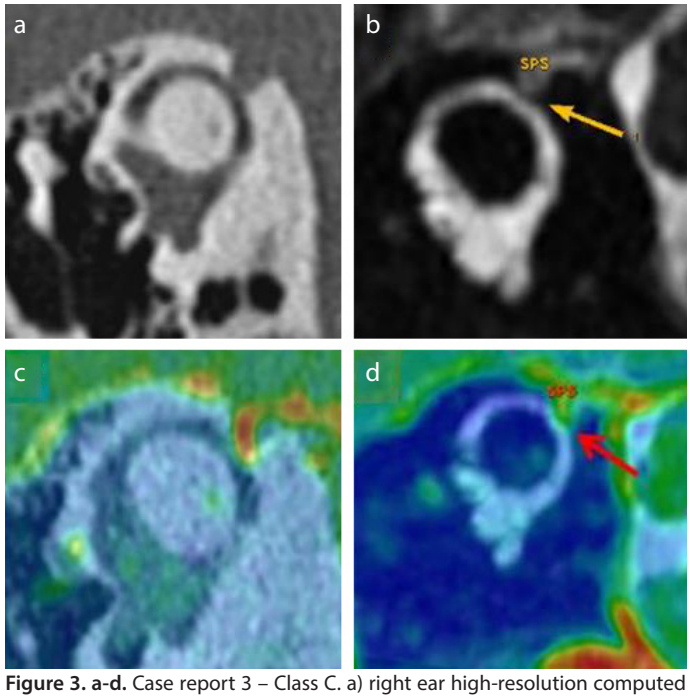

Figure 3. a-d. Case report 3 – Class C. a) right ear high-resolution computed tomography (HRCT) Pöschl plane. "Cookie bite" aspect, superior semicircular canal dehiscence (SSCD) by superior petrosal sinus (SPS) (length measured at 1.7 mm). b) T2 HR drive RMI sequence showing a labyrinthine compression. c) Fusion between HRCT and 3D T1 weighted enhanced sequence. d) Fusion between 3D T1 weighted enhanced and T2 HR FIESTA sequences. SPS compression on the SSC.

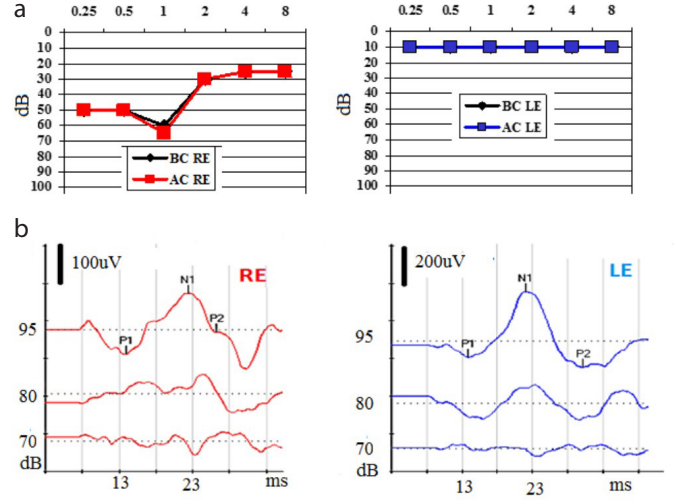

Figure 4. a, b. Case report 1. Pure tone audiometry (PTA) (a) and cervical vestibular evoked myogenic potentials thresholds (b).

Class "A" corresponds to an HRCT image with a "cookie bite" [20] and thin bone still covering the SSC (near dehiscence) in asymptomatic patients or with inner ear co-morbidities as in our case report 1 (patient presenting with clinical and audiological signs of Meniere's disease); there is no conductive hearing loss (CHL), and cVEMPs may be present with normal thresholds (Figure 1). Class "B" corresponds to a "cookie bite" image with confirmed contact between the SPS wall and the membranous SSC in MRI labyrinthine sequences; slight low frequency CHL may be present associated to cVEMPs with lower than normal thresholds on the affected side; mild to moderate clinical symptoms generally occur (patient 2, Figure 2). Class "C" type corresponds to a "cookie bite" image and obvious compression of the membranous SSC by SPS on 3T MRI sequences; cVEMPs thresholds are lower than normal and clinical signs including low frequency CHL, disabling pulsatile tinnitus, and/or imbalance or vertigo exerted by physical exercise would frequently occur (patient 3, Figure 3).

Case Report 1

A 27-year-old male patient was referred to our department for episodic vertigo associated with a right-sided hearing loss. The patient also complained of intermittent autophony and pulsating tinnitus in the right ear. PTA showed a low frequency sensorineural hearing loss (Figure 4). Vestibular assessment showed a right-sided weakness in bi-thermal caloric evaluation, according to Jonkee's formula; the VINT on the right mastoid generated instantaneously a 4°/s left horizontal nystagmus, confirming a right global vestibular deficit. Normal gains in all semicircular canals were recorded by VHIT. Low amplitude cVEMPs were present bilaterally at a normal threshold (Figure 4). The DHI and THI questionnaires revealed moderate to severe periodic impairment, which correlated with the intensity of vertiginous crisis that occurred at least 2 times/month in the past 3 months. HRCT in the right Pöschl plane showed a "cookie bite" sign with classic "near dehiscence" aspect. 3T MRI with T2 HR DRIVE sequences and fusion between HRCT and 3D T1 weighted enhanced sequences showed no contact between the SPS, although a very thin bone protecting the membranous SSC was observed (Figure 1).

In the absence of audiological and radiological arguments for OCDS by SPS, this diagnosis was ruled out. Chemical labyrinthectomy for right definite Meniere's disease by transtympanic injections of gentamicin (gentamicine Panpharma; Panpharma, Luitré, France) was therefore performed. At 6 months follow-up, he was asymptomatic and did not have another vertigo attack, although PTA confirmed decreased auditory thresholds on the affected side.

Case Report 2

A 13-year-old male child, with no previous medical history, experienced sudden vertigo, dizziness, and spatial disorientation associated with slight otalgia and moderate pulsatile tinnitus in the right ear after a scuba diving session, in which he followed all the recommended steps. Early otoscopy and otoneurological examination were normal. Standard and positional [21] PTA and speech audiometry were normal. There was no spontaneous or induced nystagmus by Valsalva or Hennebert maneuvers. Therefore, a barotraumatic oval or round window perilymphatic fistula (PLF) diagnosis was ruled out [22]. Bi-thermal caloric test was normal, and VINT elicited a vertical up-beating nystagmus although inferior to 2°/s. VHIT showed normal gain in all semicircular canals. The cVEMPs were present at low threshold (at 80 dB HL) and twice in amplitude in the right ear when compared with the left ear (Figure 5). The DHI and THI questionnaires revealed no disability, having the scores of 10 and 4, respectively. HRCT confirmed the absence of radiological signs suggesting a PLF but highlighted the presence of a right "cookie bite" aspect in the Pöschl plane. T2 HR FIESTA and fusion MRI sequences showed limited contact between SPS and membranous SSC, but no labyrinthine compression (Figure 2). A follow-up was decided with interdiction to practice scuba diving.

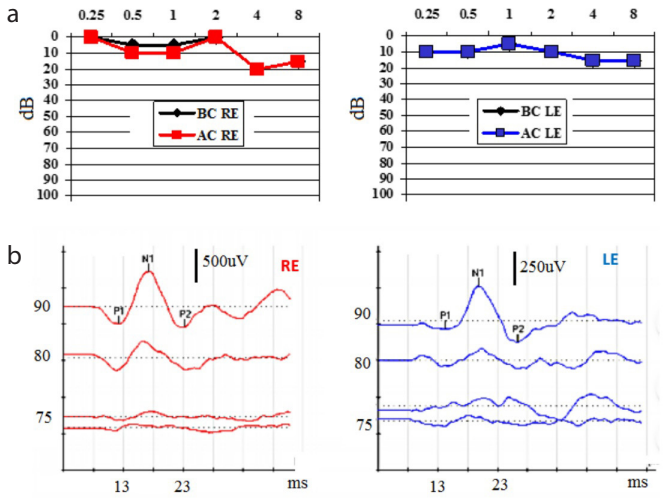

Figure 5. a, b. Case report 2. Pure tone audiometry (PTA) (a) and cervical vestibular evoked myogenic potentials thresholds (b).

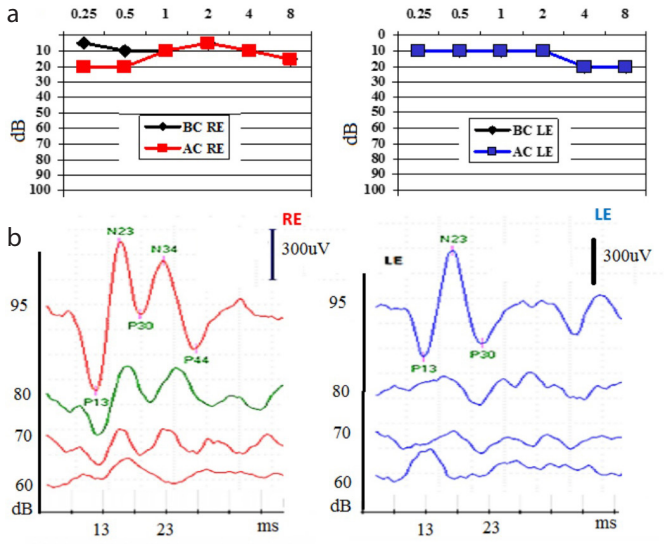

Figure 6. a, b. Case report 3. Pure tone audiometry (PTA) (a) and cervical vestibular evoked myogenic potentials thresholds (b).

Case Report 3

A 43-year-old man was referred for progressive onset of audio-vestibular symptoms. He complained of right pulsatile tinnitus, intermittent autophony, and motion-associated dizziness. PTA showed a right-sided low frequency CHL, and the vestibular assessment highlighted a right abnormally low cVEMPs threshold at 70 dB SPL (Figure 6); no other abnormality was found (i.e., VNG and VHIT were normal) except for a right beating nystagmus of 3°/s exerted by VINT. The Hennebert sign and Valsalva maneuver performed using videonystagmographic goggles did not reveal any nystagmus, although the patient experienced slight dizziness during the test. The THI questionnaire revealed a severe handicap with a high score of 80/100. HRCT of the petrous bone showed a bony defect on the right SSC limited to the groove of the SPS. Labyrinthine 3T MRI and fusion imagine techniques combined with HRCT, emphasized a compression effect of the SPS on the membranous SSC confirming the diagnosis of OCDS by vascular structure (Figure 3).

Because of worsening symptoms, the patient and multidisciplinary medical staff agreed on surgical treatment. An endovascular procedure was preferred to the classical middle fossa approach (see Ionescu et al. [16] for details of the endovascular procedure). Therefore, 2 stents were placed in the middle third of the venous structure in contact with the SSC to stiffen the SPS wall indenting the labyrinthine membrane, and 6 months after the endovascular treatment, the patient feels much better. His unsteadiness disappeared, autophony and pulsatile tinnitus significantly decreased, and the CHL disappeared; although cVEMPs still showed a lower than normal threshold at 70dB on the affected side. The THI questionnaire highlighted only a mild handicap (the score dropped to 20 points). A control by cerebral angiogram at 6 months confirmed good placement of stents and the patency of the SPS.

DISCUSSION

The goal of this study was to report 3 different clinical features (stages) in 3 patients with initially suspected SSCD by SPS only on petrosal bone HRCT basis. HRCT was systematically followed by 3T RMI labyrinthine sequences and fusion imaging procedure that highlighted the TW interface and its involved anatomical structures (e.g., the

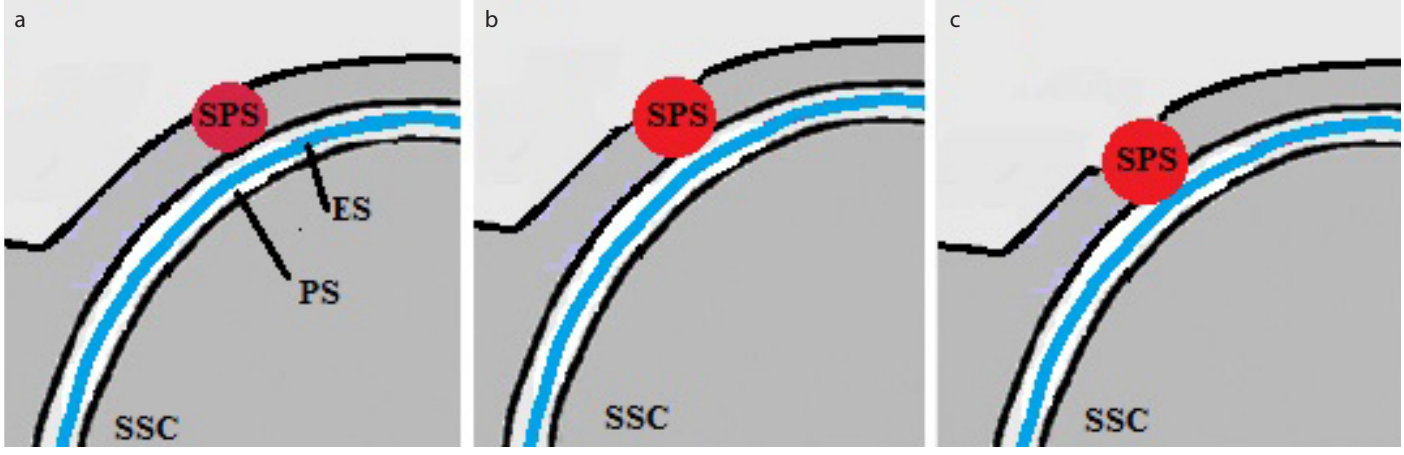

Figure 7. a-c. Schematic representation of the 3-class classification of superior semicircular canal dehiscence (SSCD) by superior petrosal sinus (SPS). a) Class A - no contact with the vestibular membrane, e.g., perilymphatic space (PS), thin bony protection still present ("near dehiscence"); b) Class B: contact with PS, a slight indentation on the PS can be observed; C: Class c) significant contact between the SPS and the vestibular membrane. Compression or stretching of the membranous SSC can be observed.

membranous SSC and the SPS). On the basis of these findings, we thought it useful to propose a 3-class classification for this vascular/vestibular dehiscence variant. This would help to select patients in the need of treatment and to choose the appropriate treatment whether surgical or endovascular.

Per previous papers [11, 14, 15, 20, 23], the most frequently reported auditory symptoms were pulsatile tinnitus and autophony; vestibular symptoms were mainly represented by motion-associated dizziness aggravated by the physical exercise. The Tullio's phenomenon was absent in all patients. Valsalva maneuver and sensitivity of the external auditory canal to the air compression (Hennebert's sign) were both negative in all patients. As previously reported [4, 7, 11], although useful for differential diagnosis (as in case report 1), vestibular assessment by VNG and VHIT was not discriminant for OCD in our series. In contrast to previous papers [17, 24], in few of our patients, the VINT appeared to be less sensitive to support an OCD diagnosis. A possible explanation would be that in this anatomic variant of OCD, the surface of the TW interface is classically limited.

Bone thinning in the upper semicircular canal could be associated with the failure of postnatal bone development [8]. In addition to specific conditions such as head trauma or barotrauma, age also appears to be an important factor in the onset of symptoms [25-26]. These data support the hypothesis that "classic" SSCD is partly an acquired condition, which may worsen with age. However, in SSCD by SPS variant, the etiology appears to be different, as the bone tissue at the margin of the SPS sulcus was found to be stable in some samples, free of a possible local osteoporosis process or similar calcium metabolic deficits [8]. In addition, we present cases of young patients with no evidence of calcium metabolic problems; this could argue for the presence of other pathophysiological mechanisms.

Clinical Elements for Therapeutic Choice

Patient 3 with MRI findings confirming a significant compression of the membranous SSC by the SPS benefited from an endovascular treatment. In this patient, the THI and DHI questionnaires indicated "catastrophic" and "severe" handicaps, respectively. After treatment, his symptoms relieved, and the result remained unchanged 2 years after, although the cVEMPS's thresholds were not "normalized." [16] This finding matches some clinical situation in patients in whom, despite having obvious radiological or audiological signs of a TW, they remain unexpectedly little or not at all symptomatic. Therefore, in our opinion, treatment aiming to reduce the abnormal transfer of acoustic energy carried by the perilymph and dissipated backward to the vestibular structures may be sufficiently effective to relieve the patient, without attempting to completely suppress or exclude the TW itself.

On the basis of our experience supported by clinical and radiological observations, in some similar patients currently followed up in our department, it appears that there is a relatively good correlation between the degree of compression by the venous structures on the membranous SSC and the intensity of symptoms.

The use of the combined HRCT and MRI and clinical classification allows for a better understanding of the clinical polymorphism of this condition and its likely pathomechanism (Figure 7). It could also help to develop future physical and/or numerical models to clarify the pathomechanism of vestibular/vascular type dehiscence, which, at the moment, is still intuitive.

Study limitations

Although our study involves a small number of patients, we propose a radio-clinical match in addition to our radiological classification in this rarer variant of SSCD. Obviously, more subjects should be included for clinical survey and treatment by endovascular approach before reinforcing these preliminary conclusions.

Possible Developments

This classification could lead to an adapted therapeutic approach. Clinical analysis, audio-vestibular assessment, THI, and DHI scores are essential and must be systematically taken into account to complete the radiological assessment before choosing the treatment. Surgery by transmastoidian or the middle fossa approach with plugging and/or capping of the SSC has been largely described [27], with variable outcomes of DHI scores [28] and auditory symptoms [28-32]. Until the endovascular approach, surgery was the only option for a curative treatment in this variant of vestibular/vascular type dehiscence.

Therefore, we can look forward to the development of therapeutic solutions, which would ensure better protection of the membranous labyrinthine structures in contact with any potentially vibratory sources causing abnormal co-stimulation of the auditory and/or vestibular end organs. A similar approach in OCDS by vascular structure was previously reported [33] to treat patients presenting with vestibular aqueduct dehiscence by the internal jugular bulb. Indeed, microinvasive techniques that could limit or eliminate the vibratory energetic transfer [5] between PS and ES would be a significant development in the treatment of these pathologies with minimal risk of audio-vestibular dysfunction.

CONCLUSION

In symptomatic patients, the combination of petrosal bone HRCT and labyrinthine 3T MRI techniques allowed for visualizing either a simple contact or a compression generated by the SPS on the membranous SSC duct. Per these criteria, we have proposed a clinical and radiological classification for this OCD variant. This would lead to a comprehensible assessment of the abnormally vibratory energy, which dissipates from the vascular wall through the audio-vestibular end organs, obviously more important in class C patients. Therefore, this classification will help in selecting patients in the need of surgical or endovascular treatment.

Ethics Committee Approval: The investigation adhered to the principles of the Declaration of Helsinki.

Informed Consent: Written informed consent was obtained from the patients who participated in this study.

Peer-review: Externally peer-reviewed.

Author Contributions: Concept – P.R., E.I., L.R. Design – P.R., E.I., L.R.; Supervision – H.T.V.; Resource – P.R., E.I., A.L.B.; Materials - P.R., E.I., A.L.B.; Data Collection and/or Processing - P.R., A.L.B.; Analysis and/or Interpretation - P.R., E.I., A.L.B.; Literature Search - E.I., P.R.; Writing - P.R., E.I., A.C.; Critical Reviews - H.T.V.

Acknowledgements: The authors thank Ruxandra Ionescu for proofreading the English.

Conflict of Interest: The authors have no conflict of interest to declare.

Financial Disclosure: The authors declared that this study has received no financial support.

REFERENCES

1. Ho ML Third Window Lesions. Neuroimaging Clin N Am 2019; 29: 57-92. [Crossref]
2. Iversen MM, Rabbitt RD. Wave Mechanics of the Vestibular Semicircular Canals. Biophys J 2017; 113: 1133-49. [Crossref]
3. Carey J, Hirvonen T, Minor L. Acoustic responses of vestibular afferents in a model of superior canal dehiscence. Otol Neurotol 2004; 25: 345-52. [Crossref]
4. Minor LB, Solomon D, Zinreich JS, Zee DS. Sound- and/or pressure-induced vertigo due to bone dehiscence of the superior semicircular canal. Arch Otolaryngol Head Neck Surg 1998; 124: 249-58. [Crossref]
5. Grieser BJ, Kleiser L, Obrist D. Identifying Mechanisms Behind the Tullio Phenomenon: a Computational Study Based on First Principles. J Assoc Res Otolaryngol 2016; 17: 103-18. [Crossref]
6. Merchant SN, Rosowski JJ. Conductive hearing loss caused by third-window lesions of the inner ear. Otol Neurotol 2008; 29: 282-9. [Crossref]
7. Wackym PA, Balaban CD, Zhang P, Siker DA, Hundal JS. Third Window Syndrome: Surgical Management of Cochlea-Facial Nerve Dehiscence. Front Neurol 2019; 10: 1281. [Crossref]
8. Carey JP, Minor LB, Nager GT. Dehiscence or thinning of bone overlying the superior semicircular canal in a temporal bone survey. Arch Otolaryngol Head Neck Surg 2000; 126: 137-47. [Crossref]
9. Lookabaugh S, Kelly HR, Carter MS, Niesten ME, McKenna MJ, Curtin H, et al. Radiologic classification of superior canal dehiscence: implications for surgical repair. Otol Neurotol 2015; 36: 118-25. [Crossref]
10. Belden CJ, Weg N, Minor LB, Zinreich SJ. CT evaluation of bone dehiscence of the superior semicircular canal as a cause of sound and/or pressure-induced vertigo. Radiol 2003; 226: 337-43. [Crossref]
11. Ward BK, Carey JP, Minor LB. Superior Canal Dehiscence Syndrome: Lessons from the First 20 Years. Front Neurol 2017; 8: 177. [Crossref]
12. Halmagy GM, McGarvie LA, Aw ST, Yavor RA,Todd MJ. The click-evoked vestibulo-ocular reflex in superior semicircular canal dehiscence. Neurology 2003; 60: 1172-5. [Crossref]
13. Zuniga MG, Janky KL, Nguyen KD, Welgampola MS, Carey JP. Ocular vs. Cervical VEMPs in the Diagnosis of Superior Semicircular Canal Dehiscence Syndrome. Otol Neurotol 2013; 34: 121-6. [Crossref]
14. Sweeney AD, O'Connell BP, Patel NS, Tombers NM, Wanna GB, Lane JI, et al. Superior Canal Dehiscence Involving the Superior Petrosal Sinus: A Novel Classification Scheme. Otol Neurotol 2018; 39: e849-55. [Crossref]
15. Özgür A, Beyazal Çeliker F, Köksal V, Beyazal M, Özdemir D, Turan, A. Radiological anatomy of superior semicircular canal and relationship to superior petrosal sinus: A study of computerized tomography. Clin Otolaryngol 2019; 44: 648-651. [Crossref]
16. Ionescu EC, Coudert A, Reynard P, Truy E, Thai-Van H, Ltaief-Boudrigua A, et al. Stenting the Superior Petrosal Sinus in a Patient with Symptomatic Superior Semicircular Canal Dehiscence. Front Neurol 2018; 9: 689. [Crossref]
17. Aw ST, Aw GE, Todd MJ, Bradshaw AP, Halmagyi GM. Three-dimensional vibration-induced vestibulo-ocular reflex identifies vertical semicircular canal dehiscence. J Assoc Res Otolaryngol 2011; 12: 549-58. [Crossref]
18. Jacobson GP, Newman CW. The development of the Dizziness Handicap Inventory. Arch Otolaryngol Head Neck Surg 1990; 116: 424-7. [Crossref]
19. Nyabenda A, Briart N, Deggouj N, Gersdorff M. Normative study and reliability of french version of the dizziness handicap inventory. Ann Readapt Med Phys 2004; 47.
20. Schneiders SMD, Rainsbury JW, Hensen EF, Irving RM. Superior petrosal sinus causing superior canal dehiscence syndrome. J Laryngol Otol 2017; 131: 593-647. [Crossref]
21. Hazell JW, Fraser JG, Robinson PJ: Positional audiometry in the diagnosis of perilymphatic fistula. Am J Otol 1992; 13: 263-9.
22. Deveze A, Matsuda H, Elziere M, Ikezono T. Diagnosis and Treatment of Perilymphatic Fistula. Adv Otorhinolaryngol 2018; 81: 133-45. [Crossref]
23. McCall AA, McKenna M J, Merchant SN, Curtin HD, Lee DJ. Superior Canal Dehiscence Syndrome Associated With the Superior Petrosal Sinus in Pediatric and Adult Patients. Otol Neurotol 2011; 32: 1312-9. [Crossref]
24. Park JH, Kim HJ, Kim JS, Koo JW. Costimulation of the horizontal semicircular canal during skull vibrations in superior canal dehiscence syndrome. Audiol Neurootol 2014; 19: 175-83. [Crossref]
25. Nadgir RN, Ozonoff A, Devaiah AK, Halderman AA, Sakai O. Superior Semicircular Canal Dehiscence: Congenital or Acquired Condition? Am J Neuroradiol 2011; 32: 947-9. [Crossref]
26. Davey S, Kelly-Morland C, Phillips JS, Nunney I, Pawaroo D. Assessment of superior semicircular canal thickness with advancing age. Laryngoscope 2015; 125: 1940-5. [Crossref]
27. Gioacchini FM, Alicandri-Ciufelli M, Kaleci S, Scarpa A, Cassandro E, Re M. Outcomes and complications in superior semicircular canal dehiscence surgery: A systematic review. Laryngoscope 2016; 126: 1218-24. [Crossref]
28. Crane BT, Minor LB, Carey JP. Superior canal dehiscence plugging reduces dizziness handicap. Laryngoscope 2008; 118: 1809-13. [Crossref]
29. Jung DH, Lookabaugh SA, Owoc MS, McKenna MJ, Lee DJ. Dizziness is more prevalent than autophony among patients who have undergone repair of superior canal dehiscence. Otol Neurotol 2015; 36: 126-32. [Crossref]
30. Koo JW, Hong SK, Kim DK, Kim JS. Superior semicircular canal dehiscence syndrome by the superior petrosal sinus. J Neurol Neurosurg Psychiatry 2010; 81: 465-7. [Crossref]
31. Alkhafaji MS, Varma S, Pross SE, Sharon JD, Nellis JC, Santina CCD, et al. Long-Term Patient-Reported Outcomes After Surgery for Superior Canal Dehiscence Syndrome. Otol Neurotol 2017; 38: 1319-26. [Crossref]
32. Bertholon P, Reynard P, Lelonge Y, Peyron R, Vassal F, Karkas A. Hearing eyeball and/or eyelid movements on the side of a unilateral superior semicircular canal dehiscence. Eur Arch Otorhinolaryngol 2018; 275: 629-35. [Crossref]
33. Thénint MA, Barbier C, Hitier M, Patron V, Saleme S, Courthéoux P. Endovascular treatment of symptomatic vestibular aqueduct dehiscence as a result of jugular bulb abnormalities. J Vasc Interv Radiol 2014; 25: 1816-20. [Crossref]